The Journal of Neuroscience, March 15, 1999, 19(6):1976–1987

Mechanisms of Calcium Influx into Hippocampal Spines: Heterogeneity among Spines, Coincidence Detection by NMDA Receptors, and Optical Quantal Analysis

Rafael Yuste,[1] Ania Majewska,[1] Sydney S. Cash,[1] and Winfried Denk[2]

[1]*Department of Biological Sciences, Columbia University, New York, New York 10027, and* [2]*Biological Computation Research Department, Bell Laboratories Lucent Technologies, Murray Hill, New Jersey 07974*

Dendritic spines receive most excitatory inputs in the vertebrate brain, but their function is still poorly understood. Using two-photon calcium imaging of CA1 pyramidal neurons in rat hippocampal slices, we investigated the mechanisms by which calcium enters into individual spines in the stratum radiatum. We find three different pathways for calcium influx: high-threshold voltage-sensitive calcium channels, NMDA receptors, and an APV-resistant influx consistent with calcium-permeable AMPA or kainate receptors. These pathways vary among different populations of spines and are engaged under different stimulation conditions, with peak calcium concentrations reaching >10 μM. Furthermore, as a result of the biophysical properties of the NMDA receptor, the calcium dynamics of spines are exquisitely sensitive to the temporal coincidence of the input and output of the neuron. Our results confirm that individual spines are chemical compartments that can perform coincidence detection. Finally, we demonstrate that functional studies and optical quantal analysis of single, identified synapses is feasible in mammalian CNS neurons in brain slices.

Key words: dendrites; spines; quantal; calcium; NMDA; hippocampus; two-photon microscopy

Dendritic spines are specialized structures that receive most excitatory synaptic inputs in mammalian neurons (Ramón y Cajal, 1904; DeRobertis and Bennett, 1955; Palay, 1956). Although there is a wealth of morphological information about dendritic spines (Harris and Kater, 1994), the exploration of their functional properties only began with the development of high-resolution calcium imaging, which allows characterization of the dynamics of free intracellular calcium concentration ($[Ca^{2+}]_i$) in spines on living neurons under a variety of physiological stimulation conditions. Imaging studies have demonstrated that spines constitute chemical compartments that partially isolate their cytoplasm from the parent dendrite (Müller and Connor, 1991; Guthrie et al., 1991; Yuste and Denk, 1995; Denk et al., 1995; Svoboda et al., 1996). This compartmentalization of calcium in spines could underlie the input specificity of synaptic plasticity (Wickens, 1988; Koch and Zador, 1993). Indeed, calcium influx into individual spines is greatly enhanced during simultaneous activation of the presynaptic and postsynaptic neuron (Yuste and Denk, 1995; Koester and Sakmann, 1998), a condition analogous to the Hebbian learning rule (Hebb, 1949). Nevertheless, the pathways of calcium entry and the biophysical mechanisms responsible for this cooperative effect are still unclear. To understand this better and to functionally characterize single, identified synaptic inputs, we measured the calcium dynamics in the spines on CA1 dendrites using two-photon fluorescence microscopy (Denk et al., 1990) under different pharmacological and stimulation conditions.

Received Nov. 4, 1998; revised Dec. 21, 1998; accepted Jan. 6, 1999.

R.Y. is funded by the Human Frontier Science Program, the EJLB Foundation, the Arnold and Mabel Beckman Foundations, and the National Eye Institute (EY 111787–01A1). We thank David W. Tank for his inspiration and generous support, Ilya Laufer and Jennifer E. Cho for help, and S. A. Siegelbaum for comments.

Correspondence should be addressed to Dr. Rafael Yuste, Department of Biological Sciences, Columbia University, 1212 Amsterdam Avenue, Box 2435, New York, NY 10027.

MATERIALS AND METHODS

Slices and electrophysiology. We used hippocampal brain slices taken from postnatal day 14–30 (P14–30) Sprague Dawley rats, and the majority of the cells were from ~P20. Therefore, our conclusions may not necessarily apply to neurons from older animals. Slices were cut with a Vibratome (TPI, St. Louis, MO), and after 1–11 hr were transferred to a submerged recording chamber. Artificial CSF (ACSF) contained (in mM): 124 NaCl, 3–5 KCl, 2 $CaCl_2$, 2 $MgSO_4$, 1.25 NaH_2PO_4, 26 $NaHCO_3$, and 10 dextrose, with 95%O_2 and 5%CO_2. APV (Sigma, St. Louis, MO), CNQX (Tocris Cookson, Bristol, UK), or $NiCl_2$ (Sigma) were sometimes also included. We recorded most data at 32°C, whereas some experiments were done at 26°C. Whole-cell recordings were made with an EPC-7 (List Electronics) or an Axoclamp 2B (Axon Instruments, Foster City, CA) amplifier operating under voltage- or current-clamp conditions. Holding V_m was −70 mV and was not corrected for junction potentials. Electrodes were filled with 135 mM K-methanesulfonate or 140 mM K-gluconate, 10 mM K-HEPES (2 mM $MgCl_2$ and 0–5 mM Na_2-ATP or 5 mM Mg-ATP), and 100–500 μM calcium green-1 or 500 μM magnesium green (Molecular Probes, Eugene, OR); resistances were ~7 MΩ. Electrophysiological signals were digitized using the second input channel of the scanning microscope or with an analog-to-digital board and Superscope (InstruNet; GW Instruments, Somerville, MA).

Two-photon imaging. CA1 pyramidal neurons were filled with calcium indicators by whole-cell perfusion. After break-in we waited ~30 min before imaging. To image the fluorescence, we used two different custom-made two-photon laser-scanning microscopes: (1) a modified Bio-Rad (Hercules, CA) MRC 600 microscope with a Ti:sapphire laser providing 100 fsec pulses at 100 MHz (830 nm wavelength; Clark MXR, Dexter, MI), pumped by an 8 W Argon ion laser source (Innova; Coherent, Santa Clara, CA), attached to a custom-built microscope using Zeiss optics with a 63×, 0.9 NA water-immersion objective (Zeiss) and (2) a modified Olympus (Melville, NY) Fluoview confocal microscope with a Ti:sapphire laser with 130 fsec pulses at 75 MHz (810 nm; Coherent), pumped by either an 8 W Argon ion laser source (Innova; Coherent) or a solid-sate pump source (Verdi; Coherent), a 40×, 0.8 NA water-immersion objective (Olympus), and optical components from Olympus and Spindler-Hoyer (Goettingen, Germany). To detect the

epifluorescence we used PMTs (Hamamatsu R3896) in external, whole-area detection mode (Denk et al., 1994), and we reconstructed the images with either COMOS (Bio-Rad) or Fluoview (Olympus) software.

Selection of spines. We imaged spines in the lower two-thirds of the stratum radiatum, located ~50–150 μm below the slice surface and at a distance 75–200 μm from the soma, as measured along the dendritic tree. Most spines were on tertiary branches. We did not notice any systematic difference among spines located at different distances from the soma.

In our experience, even with two-photon excitation, repeated imaging at high-power levels can lead to photodamage as assessed morphologically and functionally, so great care was exerted to avoid photodamage. The laser intensity was controlled with a gradient neutral density filter, and the lowest intensity necessary for an adequate signal-to-noise ratio was always used. In this paper, to exclude populations of spines with possibly compromised responses, only data are reported from neurons that met the following criteria: (1) somatic electrophysiological recordings showed resting membrane potentials more negative than −55 mV, (2) dendrites had intact morphologies without any signs of photodamage (like blebbing), and (3) calcium dynamics in spines and dendritic shafts had fast onset and decay kinetics.

Only rarely more than one spine was imaged from the same neuron. In those cases, spines were always located on different dendrites and at least 100 μm from each other. For each spine, imaging was performed during periods of at least 15 min and at most several hours, with most imaging periods lasting ~1 hour. During those periods, illumination of the sample was restricted to the minimum necessary by using a shutter (Uniblitz) controlled by a TTL pulse produced by the scanning box (Bio-Rad and Olympus).

Action potential stimulation and imaging. Action potentials were elicited by injected brief (3–50 msec) pulses of depolarizing current or voltage with the somatic electrode. The duration of the pulses was adjusted to trigger the desired number of action potentials. Although there has been recent controversy about the extent of the backpropagation of dendritic APs *in vivo* (Svoboda et al., 1997), under our experimental conditions (temperatures of 26–32°C using P14–30 rats), somatic action potentials reliably propagated to the imaged spines in stratum radiatum, as judged by the practically instantaneous (<2 msec) $[Ca^{2+}]_i$ increase in spines.

Synaptic stimulation and imaging. Synaptic stimulation was elicited by extracellular current injection using glass pipettes filled with ACSF and controlled by a pulse generator (Master-8; AMPI). Pipettes were bent to ~70° to allow vertical advancement into the slice to minimize movement of the slice and hence avoid affecting the quality of the whole-cell recording. Using custom-made electronics, we produced brief (1–3 msec) AC or DC pulses of current in either monopolar or bipolar electrode configurations and at frequencies of 20–50 Hz for short times (50–200 msec). For these experiments, we searched different dendrites from the filled neurons systematically until we were able to detect clear synaptically evoked calcium accumulations in spines. We found that to be able to elicit localized calcium transients without triggering action potentials, it was necessary to position the tip of the stimulating electrode at a close distance (~10–20 μm) from the spine. Even so, it often was not possible to elicit any significant calcium accumulations in the field of imaged spines, which normally comprised 10–40 spines while remaining below the threshold for action potential generation. This was probably a consequence of the small number (~30–50) of activated synaptic contacts that can bring the cell to threshold, together with the lack of any strict anatomical organization of individual axons in the stratum radiatum.

Analysis of calcium signals. All kinetic data were taken in the form of line scans with each time point corresponding to 2 or 2.6 msec, and each spine corresponding to ~20–50 pixels. For the analysis of calcium dynamics, we defined the fluorescence change over time as $\Delta F/F = ((F_1 - B_1) - (F_0 - B_0))/(F_0 - B_0)$, expressed in percentage, where F_1 and B_1 are fluorescence in the spine and background fluorescence, respectively, at any given time point, and F_0 and B_0 are fluorescence and background at the beginning of the experiment. Background values were taken from areas located at least 10 μm away from the spines and did not vary significantly during an experiment. In most cases $\Delta F/F$ data were filtered by smoothing 10–30 time points. Where possible, multiple traces were averaged without filtering. In experiments with poor signal-to-noise or where saturation of the indicator was suspected, quantification of $\Delta F/F$ was not performed.

Linear regression analysis of the effects of hyperpolarization on the peak calcium accumulations in spines was done by testing whether the slope of the best linear fit to all data is significantly different from the null hypothesis of zero slope. The statistic used was $T = b/SDb1$, where b = slope, and $SDb1$ = SE, using $n - 2$ degrees of freedom, where n = trial number (Moore, 1993). Linear fits of the data were obtained using Igor (Wavemetrics).

RESULTS

Action potential-induced calcium influx into spines is caused by high-threshold voltage-sensitive calcium channels

For these experiments, we studied spines in secondary and tertiary dendritic branches in stratum radiatum from 136 CA1 pyramidal neurons taken from P14–30 rats. These are the spines that mediate the most studied forms of long-term synaptic plasticity (Baudry and Davis, 1996; Fig. 1). Neurons were patched with whole-cell electrodes, filled with a calcium indicator, and changes in $[Ca^{2+}]_i$ spines were imaged with two-photon excitation under a variety of stimulation conditions.

In previous experiments we found that when a single action potential (AP) was triggered in the soma, a widespread increase in $[Ca^{2+}]_i$ occurred throughout spines and dendritic shafts in the stratum radiatum (Yuste and Denk, 1995). This indicates that action potentials antidromically invade this region of the dendritic tree (Jaffe et al., 1992; Yuste and Denk, 1995; Spruston et al., 1995b) and that, therefore, information of somatic action potential firing is immediately available to the spines. We now investigated in more detail the mechanisms of AP-induced calcium influx into spines (Fig. 2*A*). We had previously argued that calcium influx occurs in the spines because there is no delay (<2 msec) observed between the onset of spike-induced accumulations in spines or nearby dendritic shafts (Yuste and Denk, 1995). Thus, given slow intracellular diffusion of calcium (Allbritton et al., 1992) and the substantial diffusional resistance of the spine neck (Svoboda et al., 1996), the channels responsible for these accumulations have to be present on spines and dendritic shafts. We now confirmed this with new evidence showing that calcium accumulations are larger in spines than in adjacent dendritic shafts during AP stimulation, which rules out diffusion of calcium from the dendritic shaft out into the spine (four of five spines from five cells; Fig. 2*A*).

From previous work we had also concluded that the spike-induced calcium accumulations were caused by voltage-sensitive calcium channels (VSCCs) because perfusion of high concentrations (1 mM) of the VSCC blocker Ni^{2+} abolished these accumulations (Yuste and Denk, 1995). Given the fact that functional heterogeneities among spines have been demonstrated in Purkinje cells (Denk et al., 1995), we now further pursued this experiment to explore whether there were any differences among spines in this respect. In all spines tested (eight spines, eight cells; Fig. 2*B*), 1 mM Ni^{2+} abolished these accumulations without affecting action potential kinetics as determined from somatic recordings, and we thus concluded that most spines have VSCCs. To investigate which subtypes of VSCCs were responsible for the spike-induced calcium accumulations in spines, we used a lower concentration of Ni^{2+}, which has been shown to block low-voltage-activated VSCCs rather specifically (Magee et al., 1995). Under our experimental conditions, in none of the spines tested did 50 μM Ni^{2+} significantly reduce the AP-induced calcium influx (seven spines, five cells; Fig. 2*C*), even after hyperpolarizing prepulses to deinactivate low-threshold VSCC. Thus, we conclude that high-threshold VSCCs are present on most spines (as well as dendritic shafts) and that they contribute the majority of the calcium influx during action potential invasion.

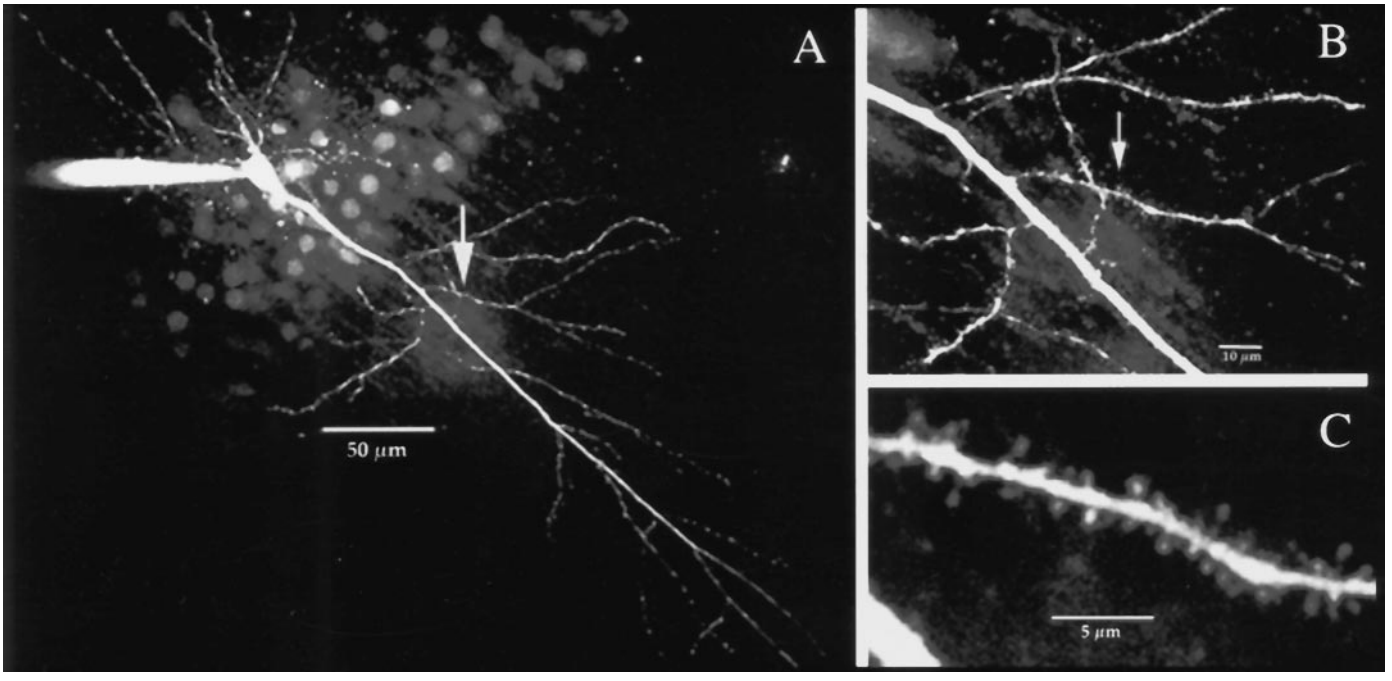

Figure 1. Two-photon imaging of dendritic spines in living hippocampal CA1 pyramidal neurons. *A*, Hippocampal CA1 pyramidal neuron filled with 200 μM calcium green. Image composed of a collapsed series of sections (2 μm apart) taken with a custom-made two-photon laser-scanning microscope. Patch pipette seen in *top left*. *Arrow* points to area shown in *B*. *B*, Field of dendrites in the radiatum shown at higher digital zoom. *Arrow* indicates region displayed in *C*. *C*, Spines on an oblique secondary dendrite ~75 μm away from the soma. Projected image is made up of a z series with 0.5 μm steps.

NMDA receptors mediate synaptically induced calcium influx into spines

To investigate the mechanisms of localized calcium accumulations that occur in individual spines in response to synaptic stimulation (Yuste and Denk, 1995), we measured calcium accumulations in spines activated by subthreshold EPSPs or EPSCs in the presence of specific blockers of glutamate receptors. In previous work we had found that simultaneous application of the NMDA receptor blocker APV (100 μM) and the non-NMDA receptor blocker CNQX (20 μM) completely abolished synaptically induced calcium influxes into spines as well as the EPSPs or EPSCs (Yuste and Denk, 1995). This demonstrated that ionotropic glutamate receptors mediate synaptically induced accumulations in spines. Metabotropic glutamate receptors alone, therefore, do not seem to be capable of mediating significant calcium accumulations in spines, although they could still play an indirect role in the synaptic response.

To reveal if these synaptically induced accumulations were caused by NMDA receptor activation, we now applied APV by itself. We found that in five of six spines from six cells (but see below), APV completely blocked synaptically induced but not AP-induced calcium accumulations (100 μM; Fig. 3). This indicates that NMDA receptors mediate most synaptically induced calcium accumulations. Because NMDA receptors are blocked by Mg^{2+} at resting potential (Nowack et al., 1984), the depolarization necessary to relieve the block could be provided by activation of AMPA receptors. Consistent with this, application of CNQX alone (20 μM) blocked synaptically induced calcium accumulations in the presence of extracellular Mg^{2+} (2 mM; two of two spines in two cells) but not in experiments performed in Mg^{2+}-free ACSF (nominally 0 mM Mg^{2+}; two of two spines in two cells). These results show that synaptically induced accumulations into spines are mostly mediated by NMDA receptors, which are blocked at rest by Mg^{2+} but presumably become unblocked by the activation of AMPA receptors during an EPSP.

Because our data showed the existence of VSCCs in the spines, we wondered whether the synaptically induced calcium increase was produced by direct calcium influx through NMDA receptors or whether it was instead caused by a secondary calcium influx through VSCCs, opened by the local depolarization of the spine caused by NMDA receptors. To evoke synaptically induced calcium influx into spines in the absence of functional VSCCs, we took advantage of the observation that long periods of whole-cell recording inactivate VSCCs (Fenwick et al., 1982; Alford et al., 1993). To accelerate the inactivation of VSCCs, we performed this series of experiments without ATP in the intracellular solution, observing that 45 min after break-in, AP-induced calcium influx into spines and dendrites completely disappeared (12 of 12 spines in 12 cells; data not shown). Under these conditions, synaptically induced calcium influx could still be reliably evoked in spines and was of comparable magnitude to that produced in neurons recorded with intracellular ATP, where VSCCs "washout" was not observed (peak amplitudes, 35 ± 15% $\Delta F/F$, $n = 5$ for spines in zero ATP vs 54 ± 30%, $n = 6$ for spines recorded in 5 mM ATP). Although we cannot rule out a residual effect caused by types of VSCCs that do not wash out or that may not produce detectable calcium accumulations during the APs (see Discussion), our results suggest that, under our experimental conditions, activation of VSCCs is not necessary for synaptically induced calcium accumulations into spines and that most of the synaptically induced calcium influx indeed occurs through NMDA receptors.

A subpopulation of spines shows APV-resistant calcium influx under synaptic stimulation

In our experiments with APV, however, we could not block the synaptically induced calcium increases in all spines. This suggests

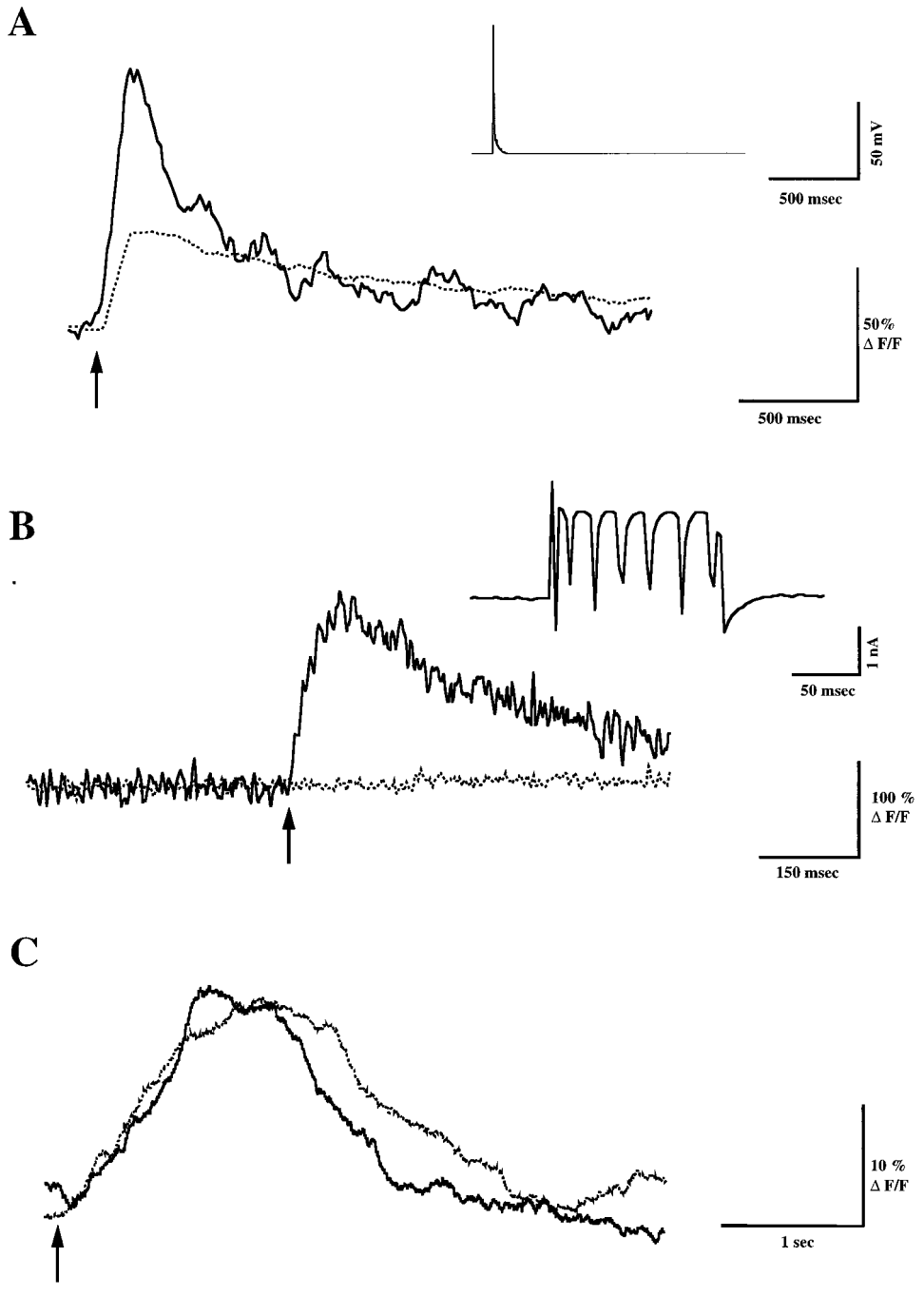

Figure 2. Mechanism of action potential-induced calcium influx into spines. *A*, Gradient of $[Ca^{2+}]_i$ between spines and dendritic shafts present during action potential-induced calcium accumulations. Fluorescence intensity changes in a dendritic spine (*solid line*) and adjacent dendritic shaft (*stippled line*) in response to a single action potential (*arrow*, *inset*). Average of five trials. The peak $\Delta F/F$ value in the dendritic spine is higher than that of the dendrite, indicating the calcium influx into the spine is local and does not diffuse in from the dendritic shaft. *B*, Calcium influx during antidromic spikes is caused by high-threshold voltage-sensitive calcium channels. *Solid line*, Fluorescence intensity changes in a dendritic spine in response to a train of action potentials (*arrow*), triggered by 50 mV, 100 msec depolarizations of the soma. *Stippled line*, After bath application of 1 mM Ni^{2+}, the calcium accumulation is completely blocked. *Inset*, Simultaneous voltage-clamp recording from the soma showing the action potentials; single trial. *C*, Low concentrations of Ni^{2+} do not affect the AP-induced calcium accumulations into spines. *Solid line*, Fluorescence intensity changes in a dendritic spine in response to a train of somatic action potentials (*arrow*; 5 Hz). *Stippled line*, The bath application of 50 μM Ni^{2+} does not significantly alter the calcium accumulation produced by the train of AP; single trial.

that a subpopulation of spines, which might also have a different functional role, have an NMDA receptor-independent pathway of calcium entry during synaptic stimulation. Only a minority of spines in the stratum radiatum appears to have this APV-resistant pathway, based on the fact that APV blocked calcium accumulations in five of six spines. To explore this issue further, we systematically searched for synaptically stimulated calcium influx into spines in the presence of APV (100 μM). Indeed, we found a population of spines where calcium influxes could be elicited synaptically in the presence of APV (Fig. 4).

This APV-resistant calcium influx could be caused by influx through VSCCs or influx through non-NMDA glutamate receptors. To distinguish between these two possibilities, we varied the holding potential to measure the membrane potential dependency of the EPSC-induced calcium accumulations under APV. Hyperpolarization removes the cell from the activation curve of VSCCs and thus reduces or eliminates calcium influx through this pathway, but the driving force for the synaptic currents and hence calcium influx through synaptic receptors is increased (Denk et al., 1995; Eilers et al., 1995). Indeed, we found that hyperpolarization increased the size of the EPSCs (Fig. 4*B*, *inset*) and in four of five spines from five cells (ages P16–21), and it also increased the calcium influx associated with synaptic stimulation (Fig. 4*C*). Because, under our experimental conditions, we could not find evidence for low-threshold VSCCs (Magee et al., 1995), such voltage dependence is inconsistent with VSCC-mediated influx. Therefore, the most likely explanation of this APV-resistant calcium accumulation is entry through a Ca^{2+}-

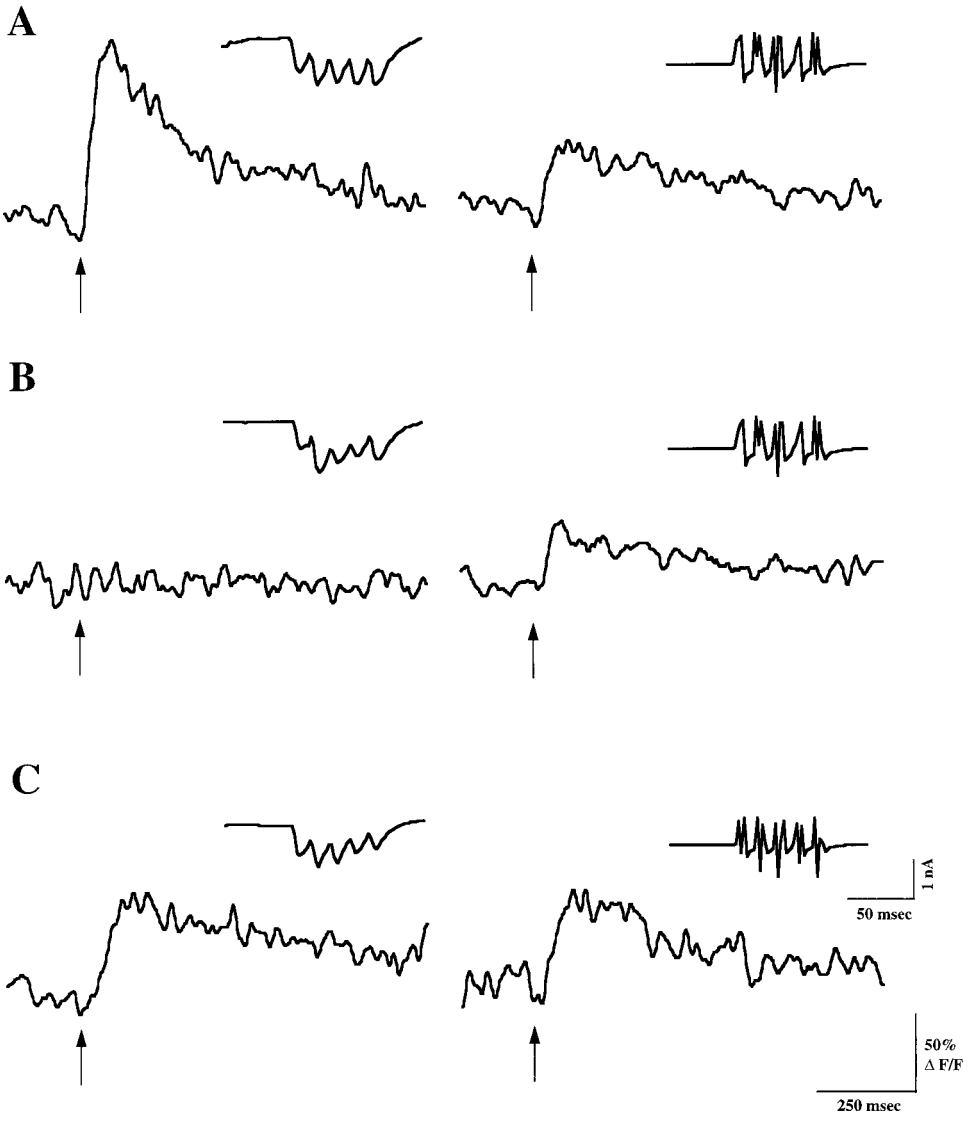

Figure 3. Mechanism of synaptically induced calcium influx into spines: APV blocks synaptically induced calcium accumulations into spines. *A*, *left*, Fluorescence intensity changes in a dendritic spine in response to a train of five EPSCs at 66 Hz (*arrow*). *Inset*, Simultaneous voltage-clamp recording from the soma. *Right*, Response of the same spine to a train of action potentials, triggered by five 50 mV, 7 msec long depolarizations of the soma (*arrow*, *inset*). *B*, *left*, In the presence of APV (100 μM), the fluorescence response to EPSCs is blocked, although the EPSCs are still present. *Right*, The spine still responds to the train of spikes. *C*, After washout of the APV, the EPSC-induced calcium influx recovers. Fluorescence data are average of three trials.

permeable glutamate receptor, probably of the AMPA or a kainate subtype. Further experiments are needed to characterize these spines in more detail.

Optical quantal analysis of synaptically induced calcium influx shows heterogeneous release probability

Under our experimental conditions it was possible to monitor the calcium accumulations at a single spine for hundreds of trials. We therefore explored the possibility of using this calcium signal from the spines to perform quantal analysis optically and to study the stochastic behaviors of calcium accumulations seen with single-shock stimuli in spines (Yuste and Denk, 1995). Unlike in electrically detected minimal stimulation experiments, optical quantal analysis assures the observation of a single synaptic contact. For the analysis of synaptic accumulations, it was useful to define the probability of obtaining a successful calcium influx after a stimulus, p_{Ca}, in analogy to the probability of release, $p_{release}$, used in quantal analysis (Katz, 1966; Jack et al., 1994). The p_{Ca} varied among spines and, under our experimental conditions (ACSF with 2 mM Ca^{2+} and 2 mM Mg^{2+}), ranged between 0.09 and 0.5. Paired-pulse stimulation increased p_{Ca} to ~0.5 (Fig. 5*A*), whereas increasing the extracellular calcium to 4 mM increased the p_{Ca} to 1 (Fig. 5*B*). These numbers are similar to estimates of $p_{release}$ derived from electrical measurements for the same synaptic pathway (Bolshakov and Siegelbaum, 1995). We conclude from the similarities between the p_{Ca} and the $p_{release}$ that the synaptically induced calcium accumulations into spines reflect of synaptic transmission and that the stochastic behavior of calcium accumulations results primarily from the stochastic nature of transmitter release.

Optical quantal analysis under minimal stimulation conditions

We never detected calcium accumulations that did not have concomitant EPSPs or EPSCs, although we often encountered failures in the p_{Ca} in the presence of EPSCs or EPSPs. This discrepancy was presumably caused by the fact that extracellular current pulses in most cases activated axons that contacted spines outside the small field of view used to achieve high time resolution. Hence, we wondered if we could activate and image a single spine under conditions of minimal stimulation, which presumably

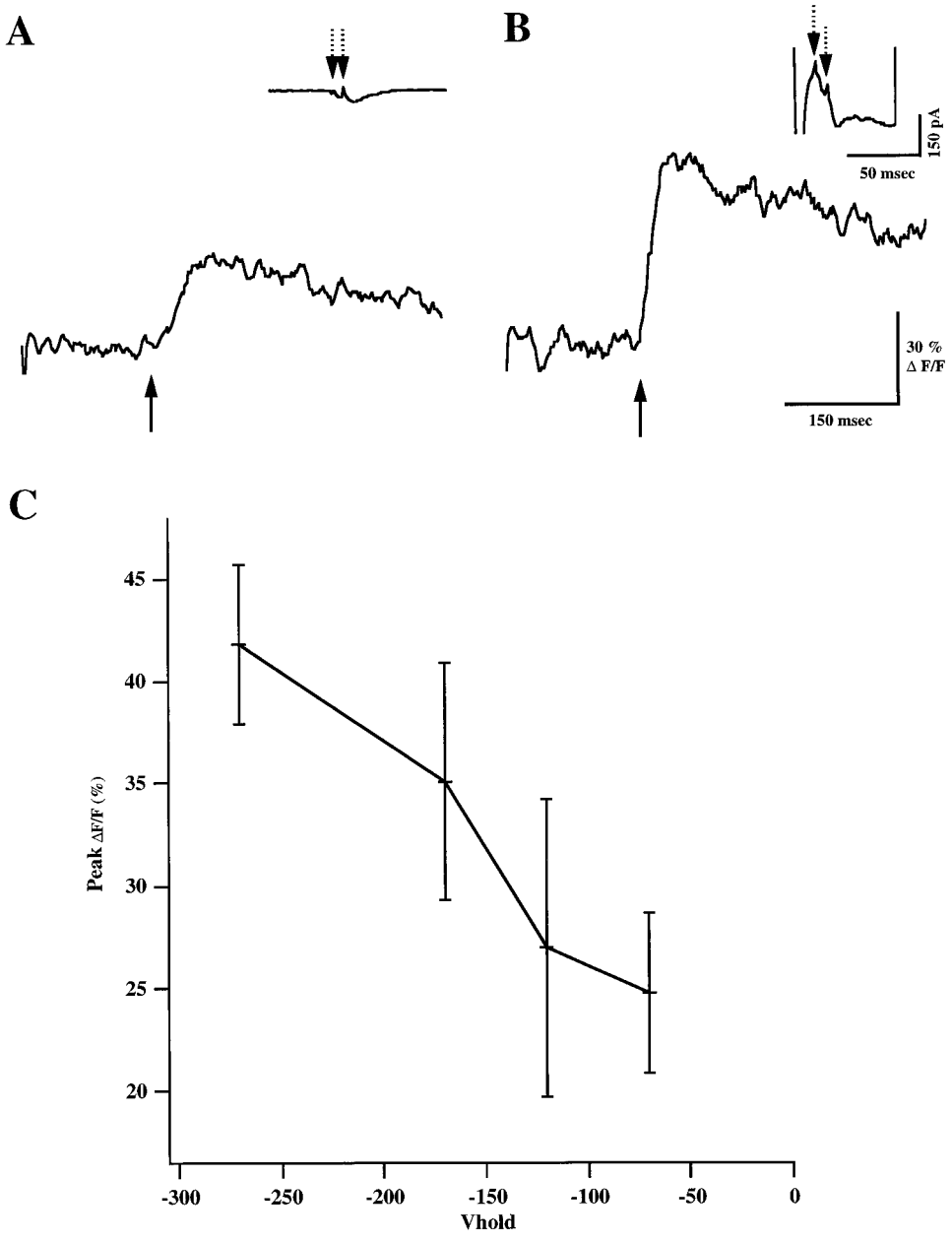

Figure 4. Mechanism of synaptically induced calcium influx into spines: APV-resistant calcium accumulations in a subpopulation of spines. *A*, Fluorescence intensity changes of a dendritic spine under 100 μM APV in response to two EPSCs at 66 Hz (*solid arrow*); average of 18 trials. *Inset* shows the simultaneous current recording at the soma during one trial. EPSCs are clearly visible (*stippled arrows*). *B*, Identical experiment during hyperpolarization of the cell to −260 mV (nominally); average of six trials. The EPSC-induced calcium influx is larger (*solid arrow*). *Inset*, The current recordings also show an enlargement of the EPSCs (*stippled arrows*), consistent with an increased EPSC driving force. Current transients before and after the response are produced by the hyperpolarization pulse. *C*, Dependence of the peak EPSC-induced calcium influx on somatic V_m. Average measurements (mean ± SEM) taken from 36 trials in one spine at four different holding potentials in the presence of 100 μM APV. Hyperpolarization of the soma produces an increase of the calcium influx into the spine (linear regression *t* test, $p < 0.02$).

only activates one axon (Raastad et al., 1992; Allen and Stevens, 1994). Thus, we lowered the stimulating current to the minimum necessary to produce distinguishable synaptic responses in our somatic recordings, while simultaneously imaging the spines located near the stimulating electrode. In one such experiment, we found a spine where calcium increases occurred only in connection to EPSCs and where failures (as mentioned above) in p_{Ca} always occurred concomitant with EPSC failures. (Fig. 6). The strict correlation (>30 trials) between calcium increase and EPSC indicates that we were indeed imaging the only spine that was being activated, because it is unlikely that other spines that could have contributed to the EPSCs had identical behavior in the stochastic $p_{release}$ as the one being imaged. Although axon failures are a theoretical possibility, they are considered unlikely (Allen and Stevens, 1994). If, as the data suggest, only the imaged spine is active, the EPSC then represents the current stemming from a single synaptic site. The peak values in the experiment shown in Figure 5*B* ranged from 2 to 7 pA and are thus in good agreement with previous estimates (Bolshakov and Siegelbaum, 1995).

Supralinear calcium increases under Hebbian pairing reach micromolar concentrations

Next, we investigated the calcium influx into spines associated with the simultaneous activation of the presynaptic and postsynaptic neurons, a condition that corresponds to Hebbian pairing. With coincident trains of EPSPs and APs, we had previously observed cooperative ("supralinear") calcium accumulations (Yuste and Denk, 1995). This supralinearity has recently also been found in layer 5 neocortical neurons by Koester and Sakmann (1998). To understand this supralinearity quantitatively, we used magnesium green, an indicator with low affinity for calcium (K_D, 6 μM in the absence of magnesium; Haugland, 1996), instead of calcium green-1, which has a high affinity (K_D, 189 nM; Haugland, 1996). At the expense of a reduced signal-to-noise

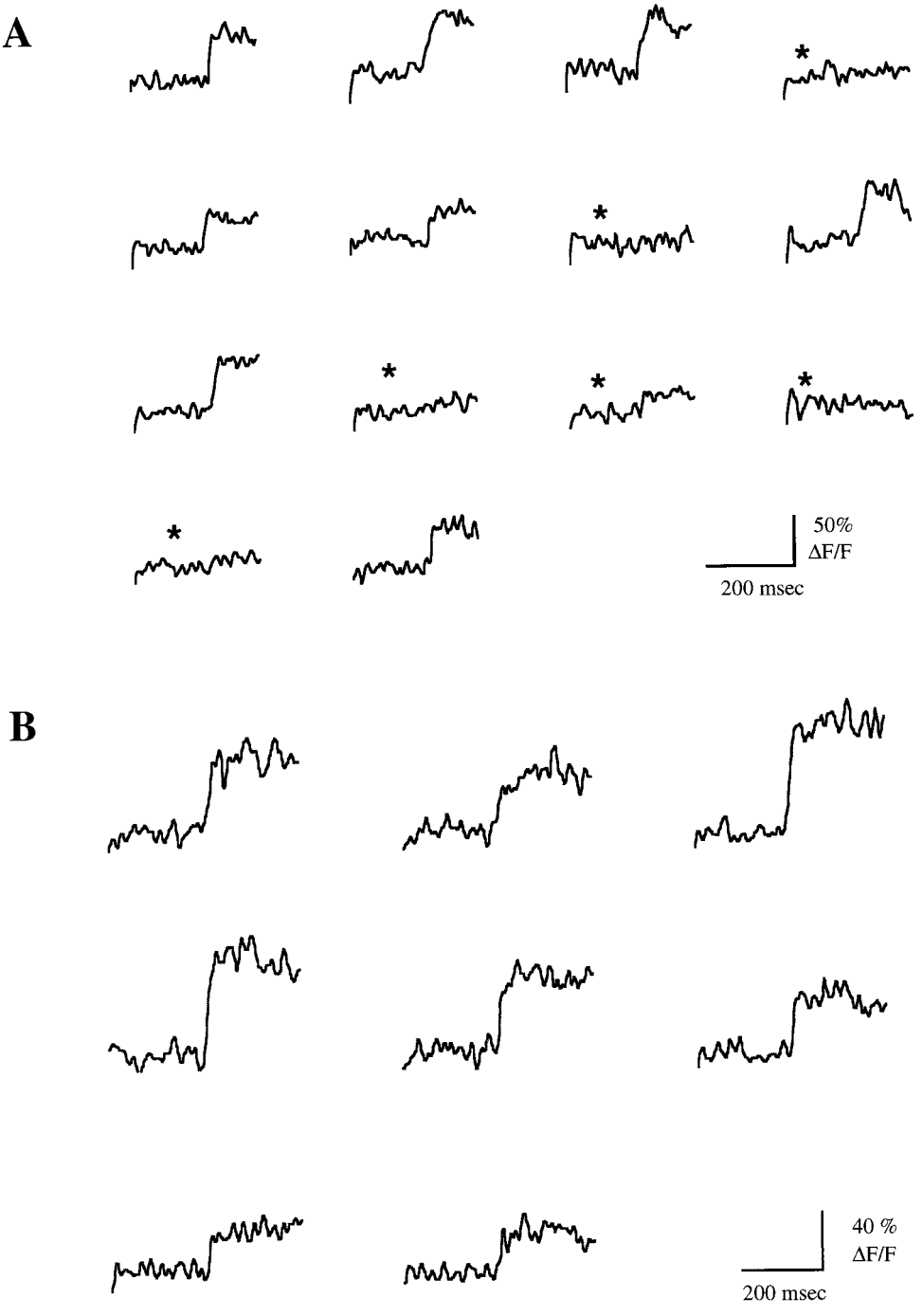

Figure 5. Changes in stochastic responses of an individual spine are apparent in the optical signal. *A*, Sequential fluorescence intensity changes in a dendritic spine in response to a paired-pulse stimulation (30 msec interval). Note how an identical stimulation protocol can elicit successes and failures (*asterisks*) in the calcium influx into spines and how approximately half of the stimuli result in a success. Responses measured in 2 mM Ca^{2+} and 2 mM Mg^{2+}. *B*, Sequential responses of the same spine to a single shock stimulation paradigm after switching to 4 mM Ca^{2+} and 1 mM Mg^{2+}. ACSF. Note the absence of failures.

ratio, a low Ca^{2+} affinity minimizes the underestimation of calcium changes that results from the saturation of the indicator at $[Ca^{2+}]$ around or above their K_D.

Indeed, with calcium green-1 we found that when a pair of closely timed APs were generated, the fluorescence change produced by the second one was smaller than that of the first one (Fig. 7*A*). This effect was caused by saturation of the indicator because both spikes produced similar increases in fluorescence when measurements were performed with magnesium green (Fig. 7*B*), suggesting that the influxes of calcium induced by each action potential are approximately equal. Combining the data taken with both indicators enabled us to calculate the absolute calcium influx contributed by each AP because as a consequence of the nonlinear dependence of fluorescence on $[Ca^{2+}]_i$, a calibration relative to the binding constant can be performed by measuring the relative fluorescence increases during to closely spaced spikes, using the following formula (Feller et al., 1996):

$$\Delta[Ca^{2+}]_i = \frac{([Ca^{2+}]_0 + K_d)(1 - \alpha)}{2\alpha}, \quad (1)$$

where

$$\alpha = \frac{(F_3 - F_2)}{(F_1 - F_0)} \quad (2)$$

and F_0 is the indicator fluorescence at resting $[Ca^{2+}]_0$, F_1 is the peak fluorescence produced by the first action potential, F_2 is the

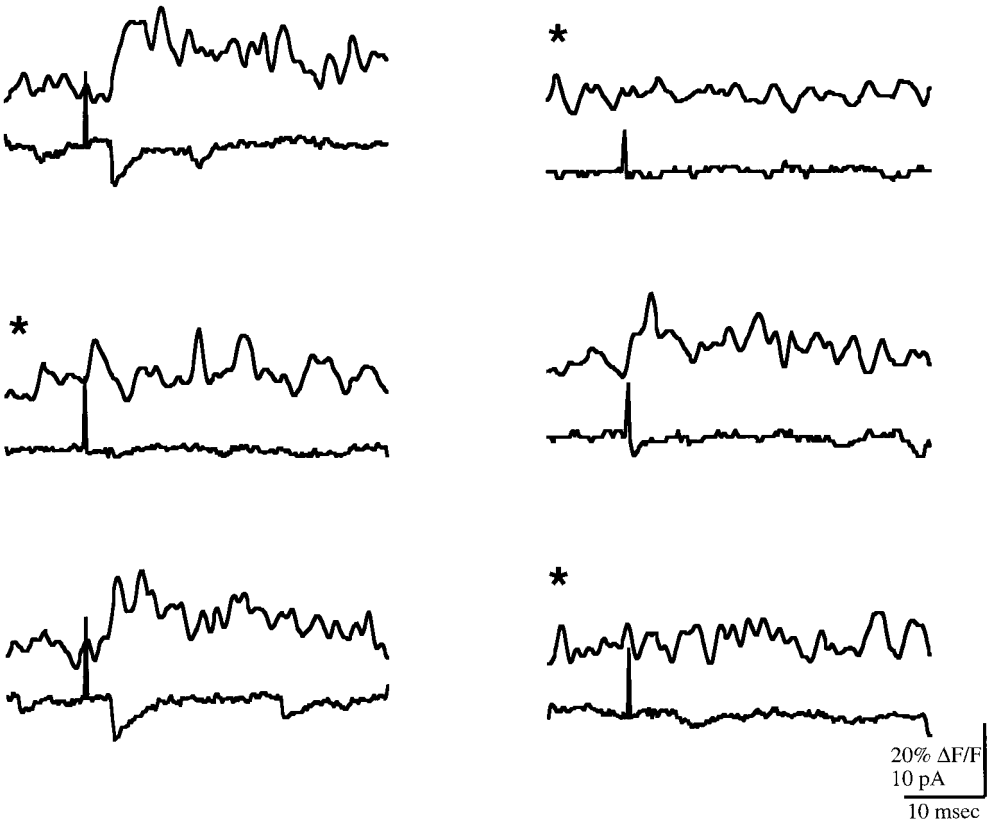

Figure 6. Optical quantal analysis of an individual spine under minimal stimulation. Fluorescence intensity changes (*top traces*) and simultaneous somatic current recordings (*bottom traces*) in a dendritic spine in response to single shock stimulation. Note the correspondence between calcium imaging of this particular spine and somatic electrophysiology: every detectable success in the calcium accumulations corresponds to a clear EPSC, whereas failures in the calcium accumulations (asterisks) are correlated with failures in the EPSCs. Responses measured in 2 mM Ca^{2+} and 2 mM Mg^{2+} ACSF.

fluorescence immediately before the second action potential, and F_3 is the peak fluorescence produced by the second action potential (Fig. 7). These equations assume, as confirmed in our case by the Mg^{2+}-green measurements, that the influxes produced by each action potential are the same and that the decay in $[Ca^{2+}]_i$ between the two action potentials is small compared with the peak $[Ca^{2+}]_i$ (Feller et al., 1996). Thus, using a resting $[Ca^{2+}]_i$ for CA1 dendrites of 75 nM (Regehr et al., 1989; Regehr and Tank, 1990), we estimated that the average $[Ca^{2+}]_i$ increase per action potential corresponds to 240 nM. Obviously this value is measured under conditions in which the calcium indicator acts as an exogenous buffer, in the case of calcium green-1 dominating the calcium buffering in the cell. We have found, in agreement with a previous report (Helmchen et al., 1996), the endogenous buffer capacity of CA1 dendrites to be ~150 (R. Yuste, D. Tank, and W. Denk, unpublished observations), which implies that the calcium influx during a single AP would raise $[Ca^{2+}]_i$ to as much as 2 μM under natural conditions (no exogenous buffer).

With magnesium green we also found, as in previous measurements with calcium green-1 (Yuste and Denk, 1995), strongly supralinear fluorescence increases (>200% compared with the arithmetic sum of the EPSPs and APs for five EPSPs and five simultaneous spikes at 66 Hz; four of four spines, four cells; Fig. 8*A*). Because the additional Ca^{2+} buffering caused by 500 μM Mg-green is only ~50% of the endogenous value, we can better estimate the $[Ca^{2+}]_i$ reached during the pairing of AP and EPSP trains as being at least 26 μM under physiological conditions (in the absence of exogenous calcium buffer). This number may still slightly underestimate the actual peak $[Ca^{2+}]_i$ reached because of saturation of magnesium green.

Timing dependency of the calcium influx supralinearity and its dependence on the NMDA receptor

The supralinearity of the calcium influx under paired synaptic and action potential stimulation of the spines suggested that the calcium concentrations reached would depend on the temporal order of sequential presynaptic and postsynaptic stimuli. To study this issue we compared stimulation protocols in which a train of three EPSPs was delivered 5 msec before a train of 2–5 spikes with trials in which the spike train preceded the EPSPs (Fig. 8*B*). The calcium increases with preceding EPSPs were much larger than for the reverse temporal order (six of six spines, four cells; Fig. 8*C*, estimated peak $[Ca^{2+}]_i$ reached ~19 μM in the absence of exogenous buffer). Both supralinearity and dependence of the total calcium influx on the temporal order were abolished by the NMDA receptor blocker APV (four of four spines, four cells; Fig. 8*D*). These results show that the "supralinear" calcium accumulations are rather sensitive to the relative timing of EPSPs and spikes and that this temporal dependency is caused by the biophysical properties of the NMDA receptor. Specifically, supralinear calcium accumulations result because the APs remove the Mg^{2+} block of the NMDA receptor, and this effect is lost if the spikes occur before the EPSPs, because Mg^{2+} unblocking of NMDA receptors is inconsequential without glutamate bound to the receptors (Nowack et al., 1984).

DISCUSSION

Parallel mechanisms of calcium influx into spines

The data presented here underscore the functional complexity of dendritic spines by revealing three different pathways for calcium influx into stratum radiatum spines from CA1 pyramidal neurons: NMDA receptors, high-threshold VSCCs, and an APV-resistant

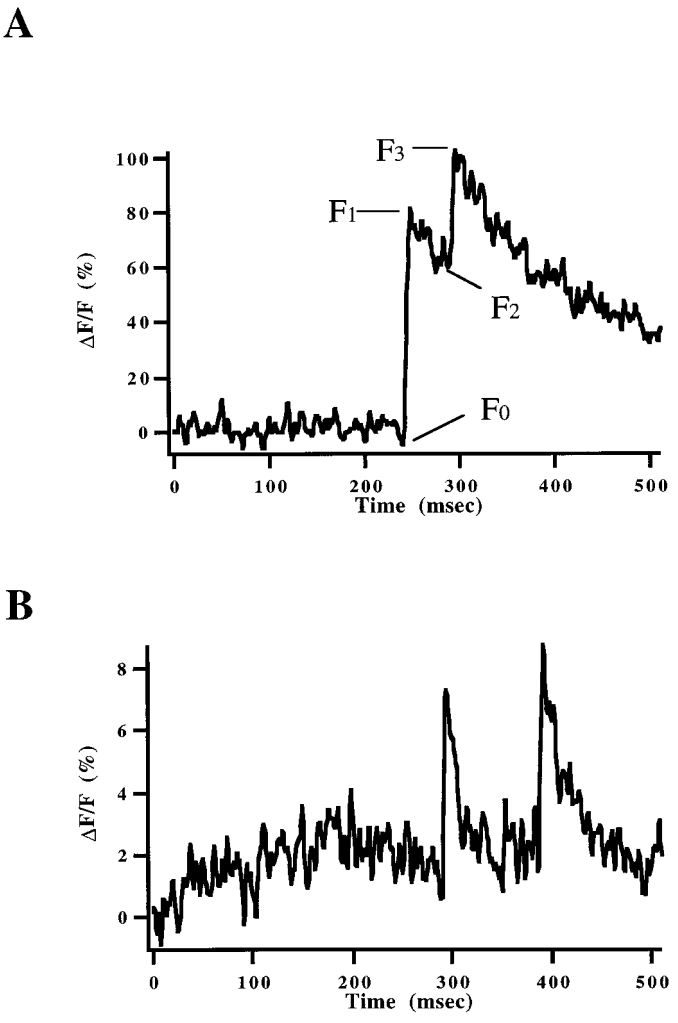

Figure 7. Quantification of action potential-induced influx. *A*, Dual action potentials reveal saturation of calcium green. Normalized changes in fluorescence of a CA1 neuron when two action potentials, 50 msec apart, are triggered through a patch pipette loaded with 500 μM calcium green. The response to the second action potential is smaller, indicative of saturation of the dye. *Letters* represent the nomenclature used in Equation 1. *B*, Lack of saturation of the response to two consecutive action potentials, 100 msec apart, in the presence of 500 μM magnesium green. Data are the average of 10 measurements. The decreased signal-to-noise ratio is caused by the lower affinity of the indicator for calcium.

pathway consistent with calcium-permeable AMPA or kainate receptors. Each pathway is activated under different conditions, with APs opening VSCCs, EPSPs activating NMDA and non-NMDA glutamate receptors, and finally, pairing of APs and EPSPs activating all pathways but with a predominance of NMDA receptors. That different physiological conditions can activate these three pathways more or less specifically suggests that they serve different functional roles and that there could be differences in the spatiotemporal $[Ca^{2+}]_i$ dynamics in a dendritic spine produced by each of these pathways. Furthermore, the exact locations of VSCCs, NMDA, and non-NMDA receptors within a spine probably differ, in particular with respect to their colocalization with other proteins. The efficiency with which calcium influx through these pathways triggers local biochemical cascades in the submembrane region, leading, for example, to synaptic plasticity, may therefore vary and not be predictable from the $[Ca^{2+}]_i$ averaged over the whole spine (Simon and Llinás, 1985). In the future this issue may be addressable with membrane-bound calcium indicators or with indicators targeted to specific molecular locations (Griffin et al., 1998).

High-threshold VSCCs in spines

The existence of VSCCs in CA1 spines and dendritic shafts was previously concluded because Ni^{2+}-sensitive calcium accumulations that occurred in spines in response to backpropagating APs did not show any delay compared with those of the nearby shafts (Yuste and Denk, 1995). Consistent with this, we now find that relative fluorescence increases ($\Delta F/F$) are larger in spines than in the adjacent dendritic shafts. Because low concentrations of Ni^{2+} do not reduce this influx, we conclude that it is probably caused by high-threshold VSCCs, without knowing the particular subtype or subtypes at this point. Our results agree with imaging data from spines in cultured hippocampal neurons (Segal, 1995), with imaging results from CA1 dendrites (Regehr and Tank, 1992), with immunocytochemical evidence suggesting that L-type high-threshold VSCCs are present in CA1 spines (Hell et al., 1996), and with patch recordings showing L-, N-, P-, Q-, and R-type channels in CA1 dendrites (Magee et al., 1995; Johnston et al., 1996). Although low-threshold or T-type VSCCs have been reported in apical dendrites in CA1 (Magee et al., 1995) and layer 5 pyramidal neurons (Markram and Sakmann, 1994), they do not appear to carry a significant fraction of the Ca^{2+} influx into stratum radiatum spines under our experimental conditions (P14–30, 26–32°C).

Existence of NMDA receptors in spines

The presence of NMDA receptors in CA1 spines has been assumed since reports of the effect of APV at the Schaffer collateral–CA1 synapse (Collingridge et al., 1983) and autoradiographic studies of the hippocampus (Monaghan et al., 1983). Further evidence came from recordings from apical dendrites showing APV-sensitive conductances (Spruston et al., 1995a), although such recordings did not sample the receptors at the synapse. Our results show that functional NMDA receptors exist in spines because localized calcium accumulations in spines, triggered by subthreshold EPSPs, are blocked by APV. This explains why such accumulations are restricted to individual spines, because only spines receiving the EPSP would contain open glutamate receptors. The restriction of $[Ca^{2+}]_i$ changes to individual spines also indicates that activation of extrasynaptic receptors is small.

Interestingly, the fact that subthreshold EPSPs produce a substantial calcium influx through the NMDA receptor into the spine even in the presence of physiological $[Mg^{2+}]$ indicates that the depolarization caused by the EPSP is sufficient to, at least partially, relieve the voltage-dependent NMDA receptor block by Mg^{2+}. That this block is only partially removed is demonstrated by the supralinear accumulation during simultaneous APs. Our observations force a modification of the simplistic view of the functional behavior of the NMDA receptors, which assumes the absence of any significant NMDA-mediated calcium influx during synaptic transmission without a substantial concomitant depolarization of the cell.

Heterogeneity in synaptically induced calcium influx among spines

We have identified a subpopulation of spines where, in APV, synaptically induced calcium influx is still detectable, indicating that, like in Purkinje cells (Denk et al., 1995), there is functional heterogeneity even among nearby spines in the stratum radiatum.

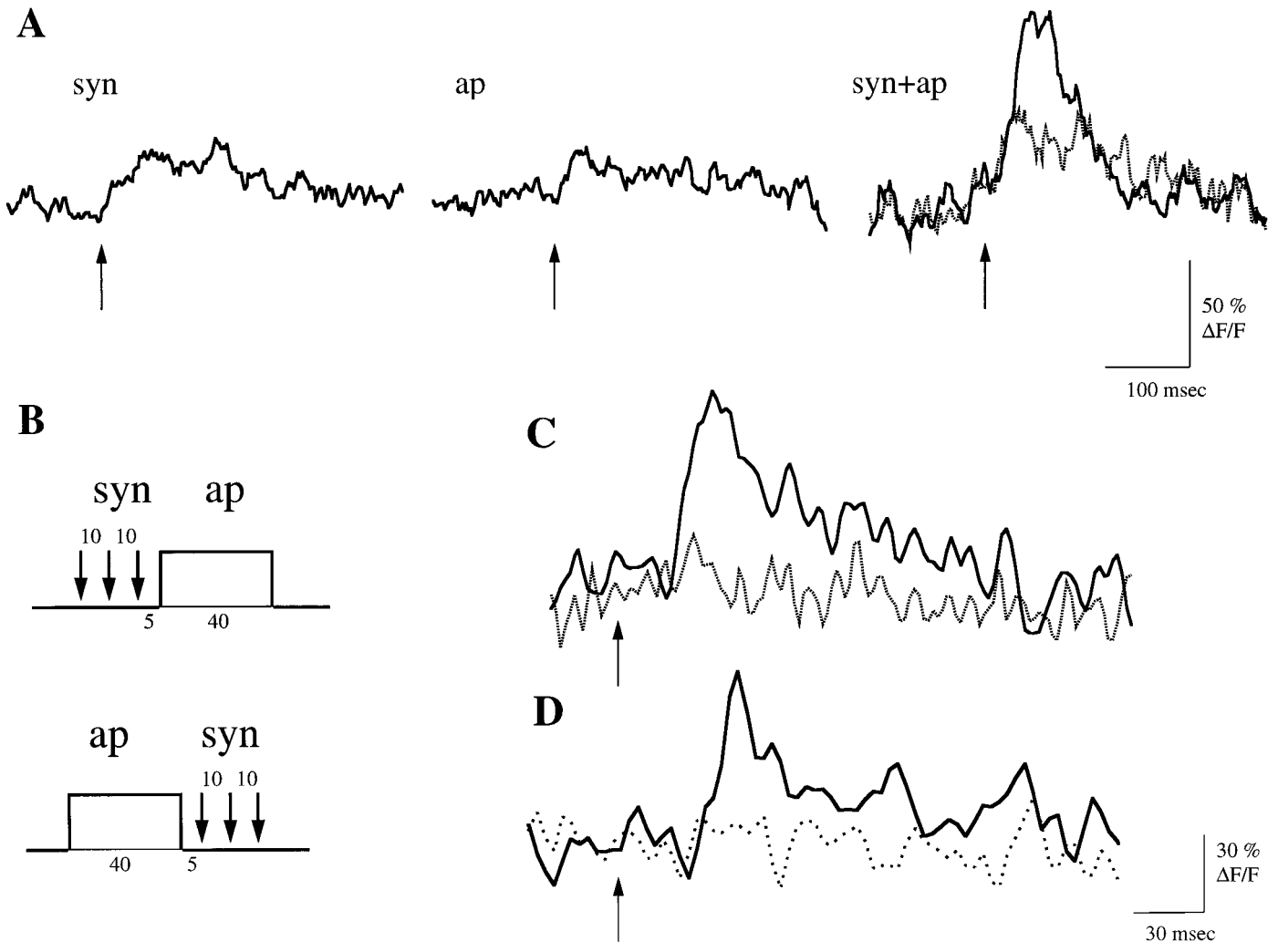

Figure 8. The supralinear calcium influx has a temporal dependency and is blocked by NMDA receptor blocker. *A*, Supralinear calcium accumulations in spines measured with magnesium green. Panels show the fluorescence intensity changes in a dendritic spine in response to a 66 Hz train of five EPSPs (*left panel*, *arrow*), five action potentials (*middle panel*), and both simultaneously (*right panel*). *Stippled line* is the arithmetic sum of the responses to the EPSPs and action potentials. Note how the actual accumulation is much larger than the expected sum; single trials. *B*, Stimulation protocol used to test the temporal dependency of the supralinearity. Three EPSPs (100 Hz) were generated 5 msec before (*top*) or after (*bottom*) a 40 msec, 50 mV depolarization that triggered two or three action potentials. *C*, The supralinearity has a temporal dependency. Fluorescence intensity changes in a dendritic spine in response to either EPSPs before (*solid line*) or after (*stippled line*) the spike train. Note how only the first condition generates any significant calcium accumulations as measured by magnesium green. Average of three trials. *D*, The supralinearity and its temporal dependency are blocked by APV. Differential fluorescence intensity changes (synaptic first minus action potentials first) in a dendritic spine in control ACSF (*solid line*) and during perfusion of 100 μM APV (*stippled line*). Note how APV blocks any significant calcium supralinearity; average of three trials.

This subpopulation of spines could reflect a different population of synapses, perhaps originating from a different axonal projection. Because of their voltage dependence, i.e., enhanced influx with hyperpolarization, Ca^{2+} entry is unlikely to be through VSCCs but must instead be directly penetrating through a glutamate receptor, which might be a Ca^{2+}-permeable AMPA receptor or a postsynaptic kainate receptor. The existence of Ca^{2+}-permeable AMPA receptors in CA1 spines is surprising given the expression of the calcium-impermeable subunit (GluR2) in rat CA1 pyramidal neurons (Geiger et al., 1995) and the lack of rectification found in dendritic recordings (Spruston et al., 1995a), although this is controversial (Lerma et al., 1994), and dendritic recordings do not sample synaptic receptors. Also, the expression of GluR2 changes with development, showing a nadir in rat CA1 at P14–21 (Pellegrini-Giampietro et al., 1992), the very ages at which our data were obtained. Finally, the presence of GluR2 in a neuron does not imply that every single AMPA receptor has a (calcium-impermeable) GluR2 subunit, and a small number of Ca^{2+}-permeable receptors (maybe only one) per spine could account for the calcium rise measured (Denk et al., 1996). An alternative possibility is that Ca^{2+} flows through kainate receptors, which are generally calcium permeable (Kohler et al., 1993), are present in CA1 (Lerma, 1997), but have not yet been described in CA1 dendrites. In this respect, it is interesting that the editing of the calcium-permeable kainate selective subunit GluR6 is also developmentally regulated in hippocampus (Schmitt et al., 1996), although the ages at which our data were collected would correspond to a high (~80%) expression of the edited subunit, which is less calcium permeable (Egebjerg and Heinemann, 1993). Further experiments are needed to characterize the identity and functional role of this subtype of spines.

Role of internal release in spines

Spines in CA1 pyramidal neurons have smooth endoplasmic reticulum and, in many cases, a spine apparatus that could release calcium from internal stores (Spacek and Harris, 1997). Consistent with this, in spines of cultured hippocampal neurons, caffeine triggers calcium increases that persist in calcium-free medium and are blocked by thapsigargin and ryanodine (Korkotian and Segal, 1988). Because the rise times of these caffeine-induced transients are significantly slower (peak at 200 msec) than those present in our measurements (in unfiltered data, AP responses can peak in <2 msec and synaptic responses can peak in <50 msec from earliest possible time of EPSP onset), we think that the initial calcium accumulations that we observe are caused by direct activation of transmembrane channels. Nevertheless, internal release, particularly calcium-induced, could well contribute to the later-phase calcium dynamics. However, except in some instances (K. Holthoff and R. Yuste, unpublished observations), we have not detected a second kinetic component, which would have allowed us to resolve the possible internal release using its kinetic signature. Alternatively, like in the sarcoplasmic reticulum, release from spine could be extremely fast, and the very high peak $[Ca^{2+}]_i$ in spines that we measured might at least partially be the result of amplification of an initial calcium influx by release from internal Ca^{2+} stores. A combination of two-photon imaging, pharmacological blockers of release, and uncaging of calcium and IP3 could be used to explore these possibilities.

Coincidence detection by NMDA receptors during Hebbian pairing

Our results demonstrate that the unblocking of NMDA receptors by APs is the mechanism of the "supralinear" calcium influx that occurs under paired APs and EPSPs (Yuste and Denk, 1995). We estimate that the calcium concentrations under these physiologically realistic pairing conditions reached levels of at least 20 μM, well into the range where enzymes like Ca^{2+}-calmodulin kinase-2 would be strongly activated. Our conclusions agree with previous tetanic stimulation experiments (Petrozzino et al., 1995) and are supported by recent experiments in neocortical neurons (Koester and Sakmann, 1998; Schiller et al., 1998). Our results also show that, using NMDA receptors, spines can detect millisecond shifts in the temporal relation between input and output of the neuron and translate the temporal structure of the stimulus into different $[Ca^{2+}]_i$. Our data thus provide support for the assumption that NMDA-mediated calcium influx into spines is involved in long-term plasticity (Miller and Kennedy, 1986; Baudry and Davis, 1996). Taken together with the effect of temporal order on synaptic plasticity (Markram et al., 1997), our results are consistent with the hypothesis that a smaller calcium influx, mediated by either VSCCs, NMDA, or Ca^{2+}-permeable AMPA or kainate receptors produces synaptic depression, whereas a larger "supralinear" calcium influx, dependent on the temporal coincidence of EPSPs and spikes and mediated mostly by NMDA receptors, could produce synaptic potentiation (Lisman, 1989).

Optical quantal analysis and functional studies of individual synapses

Finally, our data show clearly that functional studies of single, identified synaptic inputs are feasible in brain slices by combining calcium imaging of individual spines with two-photon excitation microscopy. This approach makes it possible to image single spines, and the signal-to-noise is sufficient to detect whether the spine is active or not and thus perform quantal analysis optically (Fig. 5) and also to carry out physiological and pharmacological manipulations to characterize the function of channels or receptors present at individual spines (Figs. 2–4). Optical quantal analysis can be combined with electrical recordings from the soma and minimal stimulation conditions to measure the current flowing through single spines (Fig. 6). This optical approach will enable the examination of functional properties of individual synapses in many regions of the CNS, with the advantage that the exact location of the activated synapse will be known.

REFERENCES

Alford S, Frenguelli BG, Schofield JG, Collingridge GL (1993) Characterization of the CA2+ signals induced in hippocampal CA1 neurons by the synaptic activation of NMDA receptors. J Physiol (Lond) 469:693–716.

Allbritton NL, Meyer T, Stryer L (1992) Range of messenger action of calcium ion and inositol 1,4,5-trisphosphate. Science 258:1812–1815.

Allen C, Stevens CF (1994) An evaluation of causes for unreliability of synaptic transmission. Proc Natl Acad Sci USA 91:10380–10383.

Baudry M, Davis JL (1996) Long-term potentiation, Vols 1–3, Cambridge, MA: MIT.

Bolshakov VY, Siegelbaum SA (1995) Regulation of hippocampal transmitter release during development and long-term potentiation. Science 269:1730–1734.

Collingridge GL, Kehl SJ, McLennan H (1983) The antagonism of amino acid-induced excitations of rat hippocampal CA1 neurons *in vitro*. J Physiol (Lond) 334:19–31.

Denk W, Strickler JH, Webb WW (1990) Two-photon laser scanning fluorescence microscopy. Science 248:73–76.

Denk W, Delaney KR, Gelperin A, Kleinfeld D, Strowbridge BW, Tank DW, Yuste R (1994) Anatomical and functional imaging of neurons using two photon laser scanning microscopy. J Neurosci Methods 54:151–162.

Denk W, Sugimori M, Llinás R (1995) Two types of calcium response limited to single spines in cerebellar Purkinje cells. Proc Natl Acad Sci USA 92:8279–8282.

Denk W, Yuste R, Svoboda K, Tank DW (1996) Imaging calcium dynamics in dendritic spines. Curr Opin Neurobiol 6:372–378.

DeRobertis EDP, Bennett HS (1955) Some features of the submicroscopic morphology of synapses in frog and earthworm. J Biophys Biochem Cytol 1:47–58.

Egebjerg J, Heinemann SF (1993) Ca2+ permeability of unedited and edited versions of the kainate selective glutamate receptor GluR6. Proc Natl Acad Sci USA 1993:755–759.

Eilers J, Augustine GJ, Konnerth A (1995) Subthreshold synaptic Ca2+ signalling in fine dendrites and spines of cerebellar Purkinje neurons. Nature 373:155–158.

Feller MB, Delaney KR, Tank DW (1996) Presynaptic calcium dynamics at the frog retino-tectal synapse. J Neurophysiol 76:381–400.

Fenwick EM, Marty A, Neher E (1982) Sodium and calcium channels in bovine chromaffin cells. J Physiol (Lond) 331:599–635.

Geiger JR, Melcher T, Koh D, Sakmann B, Seeburg P, Jonas P, Monyer H (1995) Relative abundance of subunit mRNAs determines gating and Ca2+ permeability of AMPA receptors in principal neurons and interneurons in rat CNS. Neuron 15:193–204.

Griffin BA, Adams SR, Tsien RY (1998) Specific covalent labelling of recombinant protein molecules inside living cells. Science 281:269–272.

Guthrie PB, Segal M, Kater SB (1991) Independent regulation of calcium revealed by imaging dendritic spines. Nature 354:76–80.

Harris KM, Kater SB (1994) Dendritic spines: cellular specializations imparting both stability and flexibility to synaptic function. Annu Rev Neurosci 17:341–371.

Haugland R (1996) Handbook of fluorescent probes and research chemicals. Eugene, OR: Molecular Probes.

Hebb DO (1949) The organization of behaviour. New York: Wiley.

Hell JW, Westenbroek RE, Breeze LJ, Wang KK, Chavkin C, Catterall WA (1996) *N*-methyl-D-aspartate receptor-induced proteolytic conversion of postsynaptic class C L-type calcium channels in hippocampal neurons. Proc Natl Acad Sci USA 93:3362–3367.

Helmchen F, Imoto K, Sakmann B (1996) Ca2+ buffering and action potential-evoked Ca2+ signalling in dendrites of pyramidal neurons. Biophys J 70:1069–1081.

Jack JB, Larkman AU, Major G, Stratford KJ (1994) Quantal analysis of the synaptic excitation of CA1 hippocampal pyramidal cells. In: Molecular and cellular mechanisms of neurotransmitter release (Stjaerne L, Greengard P, Grillner S, Hoekfelt T, and Ottoson D, eds), pp 275–299. New York: Raven.

Jaffe DB, Johnston D, Lasser-Ross N, Lisman JE, Miyakawa H, Ross WN (1992) The spread of Na spikes determines the pattern of dendritic Ca entry into hippocampal neurons. Nature 357:244–246.

Johnston D, Magee JC, Colbert CM, Christie BR (1996) Active properties of neuronal dendrites. Annu Rev Neurosci 19:165–186.

Katz B (1966) Nerve, muscle and synapse, McGraw-Hill series on the new biology. New York: McGraw-Hill.

Koch C, Zador A (1993) The function of dendritic spines: devices subserving biochemical rather than electrical compartmentalization. J Neurosci 13:413–422.

Kohler M, Burnashev N, Sakmann B, Seeburg PH (1993) Determinants of Ca2+ permeability in both TM1 and TM2 of high affinity kainate receptor channels: diversity by RNA editing. Neuron 10:491–500.

Koester, HJ and Sakmann, B (1998) Calcium dynamics in single spines during coincident pre- and postsynaptic activity depend on relative timing of back-propagating action potentials and subthreshold excitatory postsynaptic potentials. Proc Natl Acad Sci USA 95:9596–9601.

Korkotian E, Segal M (1988) Fast confocal imaging of calcium released from stores in dendritic spines. Eur J Neurosci 10:2076–2084.

Lerma J (1997) Kainate reveals its targets. Neuron 19:1155–1158.

Lerma J, Morales M, Ibarz JM, Somohano F (1994) Rectification properties and Ca2+ permeability of glutamate receptor channels in hippocampal cells. Eur J Neurosci 6:1080–1088.

Lisman J (1989) A mechanism for the Hebb and anti-Hebb processes underlying learning and memory. Proc Natl Acad Sci USA 86:9574–9578.

Magee JC, Christofi G, Miyakawa H, Christie B, Lasser-Ross N, Johnston DJ (1995) Subthreshold synaptic activation of voltage-gated Ca2+ channels mediates a localized Ca2+ influx into the dendrites of hippocampal pyramidal neurons. J Neurophysiol 74:1335–1341.

Markram H, Sakmann B (1994) Calcium transients in apical dendrites evoked by single sub-threshold excitatory post-synaptic potentials via low voltage-activated calcium channels. Proc Natl Acad Sci USA 91:5207–5211.

Markram H, Luebke J, Frotscher M, Sakmann B (1997) Regulation of synaptic efficacy by coincidence of postsynaptic APs and EPSPs. Science 275:213–215.

Miller SG, Kennedy MB (1986) Regulation of brain type II Ca2+/calmodulin-dependent protein kinase by autophosphorylation: a Ca2+-triggered molecular switch. Cell 44:861–870.

Monaghan DT, Holets VR, Toy DW, Cotman CW (1983) Anatomical distributions of four pharmacologically distinct 3H-L-glutamate binding sites. Nature 1983:176–179.

Moore DS (1993) Introduction to the practice of statistics. New York: Freeman.

Müller W, Connor JA (1991) Dendritic spines as individual neuronal compartments for synaptic Ca2+ responses. Nature 354:73–76.

Nowack L, Bregestovski P, Ascher P, Herbet A, Prochiantz A (1984) Magnesium gates glutamate-activated channels in mouse central neurons. Nature 307:462–465.

Palay SL (1956) Synapses in the central nervous system. J Biophys Biochem Cytol 2:193–201.

Pellegrini-Giampietro DE, Bennet MVL, Zukin RS (1992) Are Ca2+-permeable kainate/AMPA receptors more abundant in immature brain? Neurosci Lett 144:65–69.

Petrozzino JJ, Pozzo Miller LD, Connor JA (1995) Micromolar Ca2+ transients in dendritic spines of hippocampal pyramidal neurons in brain slice. Neuron 14:1223–1231.

Raastad M, Storm JF, Andersen P (1992) Putative single quantum and single fibre excitatory postsynaptic currents show similar amplitude range and variability in rat hippocampal slices. Eur J Neurosci 4:113–117.

Ramón y Cajal S (1904) La textura del sistema nerviosa del hombre y los vertebrados. Madrid: Moya.

Regehr WG, Tank DW (1990) Postsynaptic NMDA receptor-mediated calcium accumulation in hippocampal CA1 pyramidal cell dendrites. Nature 345:807–810.

Regehr WG, Tank DW (1992) Calcium concentration dynamics produced by synaptic activation of CA1 hippocampal pyramidal cells. J Neurosci 12:4202–4223.

Regehr WG, Connor JA, Tank DW (1989) Optical imaging of calcium accumulation in hippocampal pyramidal cells during synaptic activation. Nature 341:533–536.

Schiller J, Schiller Y, Clapham DE (1998) NMDA receptors amplify calcium influx into dendritic spines during associative pre- and postsynaptic activation. Nat Neurosci 1:114–118.

Schmitt J, Dux E, Gissel C, Paschen W (1996) Regional analysis of developmental changes in the extent of GluR6 mRNA editing in rat brain. Brain Res Dev Brain Res 91:153–157.

Segal M (1995) Fast imaging of $[Ca]_i$ reveals presence of voltage-gated calcium channels in dendritic spines of cultured hippocampal neurons. J Neurophysiol 74:484–488.

Simon SM, Llinás RR (1985) Compartmentalization of the submembrane calcium activity during calcium influx and its significance in transmitter release. Biophys J 48:485–498.

Spacek J, Harris KM (1997) Three-dimensional organization of smooth endoplasmic reticulum in hippocampal CA1 dendrites and dendritic spines of the immature and mature rat. J Neurosci 17:190–203.

Spruston N, Jonas P, Sakmann B (1995a) Dendritic glutamate receptor channels in rat hippocampal CA3 and CA1 pyramidal neurons. J Physiol (Lond) 482:325–352.

Spruston N, Schiller Y, Stuart G, Sakmann B (1995b) Activity-dependent action potential invasion and calcium influx into hippocampal CA1 dendrites. Science 286:297–300.

Svoboda K, Tank DW, Denk W (1996) Direct measurement of coupling between dendritic spines and shafts. Science 272:716–719.

Svoboda K, Denk W, Kleinfeld D, Tank DW (1997) *In vivo* dendritic calcium dynamics in neocortical pyramidal neurons. Nature 385:161–165.

Wickens J (1988) Electrically coupled but chemically isolated synapses: dendritic spines and calcium in a rule for synaptic modification. Prog Neurobiol 31:507–528.

Yuste R, Denk W (1995) Dendritic spines as basic units of synaptic integration. Nature 375:682–684.